

DOI: <http://dx.doi.org/10.21123/bsj.2017.14.2.0427>

Analysis and Study of the Effect of Atmospheric Turbulence on Laser weapon in Iraq

Lecturer Thair Abdulkareem Khalil Al-Aish

Department of Physics, College of Education for Pure Sciences Ibn Al-Haitham, University of Baghdad, Baghdad, Iraq.

E-mail: dr.thair.73@gmail.com

Received 1/9/2016

Accepted 30/11/2016



This work is licensed under a [Creative Commons Attribution 4.0 International License](https://creativecommons.org/licenses/by/4.0/)

Abstract:

One of the most important challenges facing the development of laser weapons is represented by the attenuation of the laser beam as it passed through the layers of atmosphere.

This paper presents a theoretical study to simulate the effect of turbulence attenuation and calculates the decrease of laser power in Iraq. The refractive index structure C_n^2 is very important parameter to measure the strength of the atmospheric turbulence, which is affected by microclimate conditions, propagation path, season and time in the day.

The results of measurements and predictions are based on the Kolmogorov turbulence theory. It was demonstrated by simulations that the laser weapons in Iraq were severely affected due to the large change in temperatures, the limited effective range of laser weapon to a few kilometers as a result of high attenuation and the middle of stratosphere considered as a homogeneous and a suitable area for the work of laser weapons, so be a favorite area of fighter aircraft.

Key words: turbulence attenuation, Laser Weapon, refractive index structure C_n^2 , Fried parameter r_0 , Beam divergence.

Introduction:

The atmosphere around the globe is composed of a diverse mass of which gravitate toward the earth's surface by gravity. The importance of the atmosphere is as follows [1,2]:

- It protects life on Earth by UV absorption

- Surface warming through the greenhouse effect
- To attenuate the power of sunlight falling on the earth's surface and reduce the temperature.

The International Standard Atmosphere (ISA) and properties of it at mean sea level (MSL) is shown in Table 1[2].

Table (1): Properties of atmosphere

Composition	Layers	Temperature T ₀	Pressure P ₀	Density ρ ₀	Mass M ₀
Nitrogen 78.09%	Troposphere 0 To 11 Km	288.15 K	101325 N/M2	1.225 Kg/M3	5.15×10 ¹⁸ Kg
Oxygen 20.95%	Stratosphere 11 To 50 Km				
Argon 0.93%	Mesosphere 50 To 80 Km				
Carbon Dioxide 0.039%	Thermosphere 80 To 700 Km				
Water Vapor 0.4 - 1 %	Exosphere 700 To 10,000 Km				

The beam of laser weapons can be affected by the atmosphere layers when it propagates through it. The attenuation due to absorption, scattering, thermal blooming and turbulence, changing the power of the beam as well as beam wander and beam breakup [3].

The quality of the laser beam is determined by interactions with the atmospheric species and aerosol particles. The value of beam power at the target is a measure of this quality[4]. The turbulence of laser beam arises as a result of the heterogeneity of atmosphere layers, causing temporal and spatial fluctuations of direction propagation, spot dancing, beam spread and scintillations.

This work is limited to the study and analysis the effect of turbulence attenuation on the beam of laser weapon.

Theory of Atmospheric turbulence

The gradient in temperature (positive or negative) between the surface of the earth and the atmosphere leads to the generation of so-called air turbulence. Since the Earth's surface during the daytime will be at higher temperature than the air above, a negative gradient will causes a difference in refractive index values, beam direction (according to the Snell's Law) refraction upward with angle depends on strong gradient. At nighttime, the gradients are positive

which causes the beam direction refraction downward. [2]

To calculate temperature (T), pressure (P) and density (ρ) as a function of the altitude in meter, the Standard model of Atmosphere was used to calculate the temperature (T), pressure (P) and density (ρ) within the troposphere layer. Temperature decreases with altitude at a constant rate of -6.5 K /km up to the troops (Border line between the troposphere and the stratosphere). The standard tropopause altitude is 11 km. The (ISA) temperature model within the troposphere is: [2,4]

$$T = T_0 - 0.0065 h \dots\dots (1)$$

From 11 to 20 km, the change of temperature is 0 K/km, but from 20 to 32 km the change is 1 K/km. The ISA pressure model within the troposphere is [4]:

$$P = P_0 \left(1 - 0.0065 \frac{h}{T_0} \right)^{5.2561} \dots\dots (2)$$

$$\frac{P}{P_0} = \left(\frac{T}{T_0} \right)^{5.256} \dots\dots(3)$$

$$\frac{\rho}{\rho_0} = \left(\frac{T}{T_0} \right)^{4.256} \dots\dots (4)$$

The temperature is constant at altitudes above the tropopause, the ISA pressure model become:

$$P = P_{11} e^{-\frac{g}{RT_{11}}(h-h_{11})} \dots (5)$$

Where the parameters with subscript "11" correspond to the values at the tropopause (P₁₁ = 226.32 N/m², T₁₁ = 216.65 K, h₁₁ = 11 km) and R universal gas constant 8.31447 J/(mol•K). (Earth-surface gravitational acceleration 9.80665 m/s²). In the

middle stratosphere, the pressure and density are given by [2.4]:

$$\frac{P}{P_{20}} = \left(\frac{T}{T_{20}}\right)^{-34.1632} \dots\dots(6)$$

$$\frac{\rho}{\rho_{20}} = \left(\frac{T}{T_{20}}\right)^{-35.1632} \dots\dots(7)$$

The variations of temperature and wind velocity create unstable air mass called turbulent eddies. Eddies can occur in the whole path propagation of the laser beam as different scale sizes from a micro scale to a macro scale. That's mean, variance in the refraction index depends on the local temperature, atmospheric pressure or particle density [5,6].

The refractive index *n* is a function of temperature *T* (in Kelvin), pressure *P* (in mbar) and wavelength of laser weapon (in this work ($\lambda = 1.075 \mu\text{m}$)). The index of refraction, neglecting water vapor pressure, is given by: [6]

$$n = 1 + \frac{77.6 P_r}{T} \times 10^{-6} \left[1 + \frac{0.00753}{\lambda^2}\right] \dots\dots(8)$$

For laser weapons systems, the coherence of the laser beam is very important for the propagation of laser energy through the atmosphere layers, so that they constructively interfere to form a high irradiance spot size on target. In addition, the constructive interference will disrupt as a result of the variations in refractive index due to turbulence [6,7].

The index-of-refraction structure parameter C_n^2 (in units of $\text{m}^{-2/3}$) is used to measure the strength of the turbulence. Andrey Kolmogorov was the first theoretically parameterized. Kolmogorov's theory utilizes a statistical approach in describing the flow of kinetic energy from large-scale eddies (about 10's of meters to 1cm in size). Eddy is defined as relatively homogeneous and isotropic within smaller regions of space, This assumption is allowed for Kolmogorov

to utilize C_n^2 to measure the strength of the turbulence. The related structure function exhibits asymptotic behavior [5,6]

$$D_n(R) = \begin{cases} C_n^2 R^{2/3} & , l_0 \ll R \ll L_0 \\ C_n^2 l_0^{-4/3} R^2 & , R \ll l_0 \end{cases} \dots\dots(9)$$

Where *R* is scalar distance, L_0 is the outer scale of turbulence and l_0 is the inner scale of turbulence. C_n^2 is a defined as the mean-square difference in the refractive index at two locations divided by the distance *r* raised to the 2/3 power, i.e., [5,6]

$$C_n^2 = \frac{\langle(n_2 - n_1)^2\rangle}{R^{2/3}} \dots\dots\dots(10)$$

The other important quantity used to describe turbulence of the propagating laser beam is Fried parameter r_0 in (m), which represents an atmospheric coherence diameter. The r_0 parameter is a circular diameter over the laser beam which maintains coherence in the propagation distance. A lower r_0 value implies stronger turbulence. If the r_0 value is significantly smaller than the laser beam director size, the laser beam will break up into many smaller, incoherently radiating beam. The relation between r_0 , C_n^2 , λ , and the distance to target *d* can be given by [8,9,10]:

$$r_0 = 0.33 \frac{\lambda^{6/5}}{(d^{3/5} C_n^2)^{3/5}} \dots\dots(11)$$

The power of laser weapon (*P*) on target through the earth's atmosphere which can be calculated by [9,11]:

$$P = \frac{AP_t}{d^2 R_s^2} e^{-\epsilon d} \dots\dots(12)$$

Where P_t represents the total output power from the laser weapon (100 kw), R_s area of spot size at target *A* is area of spot size at weapon, ϵ is the total extinction coefficient due to atmospheric, absorption and scattering (in m^{-1}) and *d* represents the distance to target [12,13].

$$\epsilon = \frac{3.912}{d} \left(\frac{0.55}{\lambda}\right)^q \dots\dots(13)$$

The value of q depends on the range of laser weapon, when $d \leq 6 \text{ km}$ q is given by $0.585 (d)^{1/3}$ and when $6 \text{ km} < d < 50 \text{ km}$ q is equal to 1.3.

The effect of turbulence on the laser spot size R_s On target can be estimated by [9,14,15]:

$$R_s \approx \frac{\lambda d}{\pi r_0} \dots\dots(14)$$

Where d represents the distance to target and the Fried parameter r_0

Results and Discussion:

In this paper, the results were obtained by simulation using Matlab software. The effectiveness of laser weapons can be greatly affected by the layers of atmosphere. Table 1 shows the

properties of atmosphere and international Standard Atmosphere ISA assumes the mean sea level MSL condition.

Table 2 clearly shows the atmospheric turbulence, generated by a temperature differential between the Earth’s surface and the atmosphere. Fig (1) shows that the temperature T (K) decreases with altitude h (km) at a constant rate of -6.5 K /Km (Eq.1) in the troposphere layer, then T remains at a constant value of 216.65 K from Stratosphere layer up to 20 km. Then, the temperature increases at a rate of one degree up to 32 km (middle of the stratosphere).

Table (2): Shows the data of various parameters, generated by a temperature differential between the Earth’s surface and the atmosphere

h(km)	T(k)	P(mbar)	$\rho(\frac{\text{kg}}{\text{m}^3})$	N	$C_n^2 (\text{m}^{-2/3})$	$r_0(\text{m})$
0 msl	288.15	1013.25	1.225	1.0002749	6.48×10^{-12}	0.00975
1	281.65	898.74	1.111	1.0002495	5.59×10^{-12}	0.01065
2	275.15	794.94	1.006	1.0002259	4.81×10^{-12}	0.01166
3	268.65	701.08	0.909	1.0002040	4.09×10^{-12}	0.012857
4	262.15	616.39	0.819	1.0001838	3.47×10^{-12}	0.01419
5	255.65	540.19	0.736	1.0001652	2.97×10^{-12}	0.01557
6	249.15	471.8	0.659	1.0001480	2.47×10^{-12}	0.01740
7	242.65	410.6	0.589	1.0001323	2.11×10^{-12}	0.01912
8	236.15	355.99	0.525	1.0001178	1.75×10^{-12}	0.02139
9	229.65	307.41	0.466	1.0001046	1.44×10^{-12}	0.02405
10	223.15	264.35	0.412	1.0000926	1.21×10^{-12}	0.02670
11	216.65	226.31	0.363	1.0000816	1.42210×10^{-12} End of Troposphere	
12	216.65	193.3	0.310	1.0000697	10.40×10^{-13}	0.02924
13	216.65	165.1	0.265	1.0000595	7.60×10^{-13}	0.03529
14	216.65	141.01	0.226	1.0000508	5.50×10^{-13}	0.04285
15	216.65	120.44	0.193	1.0000434	3.98×10^{-13}	0.05203
16	216.65	102.87	0.165	1.0000371	2.92×10^{-13}	0.06265
17	216.65	87.86	0.141	1.0000317	2.21×10^{-13}	0.07405
18	216.65	75.04	0.120	1.0000270	1.50×10^{-13}	0.09344
19	216.65	64.1	0.103	1.0000231	11.61×10^{-14}	0.10896
20	216.65	54.74	0.088	1.0000197	8.74×10^{-14}	0.12921
21	217.65	46.77	0.074	1.0000168	6.79×10^{-14}	0.15034
22	218.65	39.93	0.061	1.0000142	4.43×10^{-14}	0.19425
23	219.65	34.22	0.054	1.0000121	3.25×10^{-14}	0.23392
24	220.65	29.3	0.046	1.0000103	2.26×10^{-14}	0.29089
25	221.65	25.10	0.039	1.0000088	1.69×10^{-14}	0.34631
26	222.65	21.53	0.033	1.0000075	1.21×10^{-14}	0.42318
27	223.65	18.47	0.028	1.0000064	8.31×10^{-15}	0.53020
28	224.65	15.86	0.024	1.0000055	6.42×10^{-15}	0.61898
29	225.65	13.62	0.021	1.0000047	4.92×10^{-15}	0.72614
30	226.65	11.71	0.018	1.0000040	3.61×10^{-15}	0.87437
31	227.65	10.08	0.015	1.0000034	2.51×10^{-15}	1.08742
32	228.65	8.67	0.013	1.0000029	1.39×10^{-15}	1.23565

The pressure P(mbar) and density $\rho (\frac{\text{kg}}{\text{m}^3})$ Varies with altitude

h (km) depending on Eqs.3, 4,5,6,7 as shown in Figs. 2,3. It can be shown the P and ρ drops exponentially with

increasing altitude above mean sea level MSL; this is because most of the atmospheric mass is concentrated in a troposphere layer (It contains approximately 75% of the atmosphere's mass and 99% of its water vapor and aerosols).

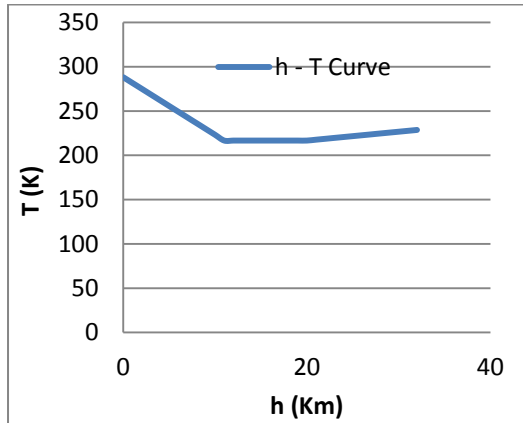


Fig (1) shows the temperature differential between the Earth's surface and the atmosphere layers.

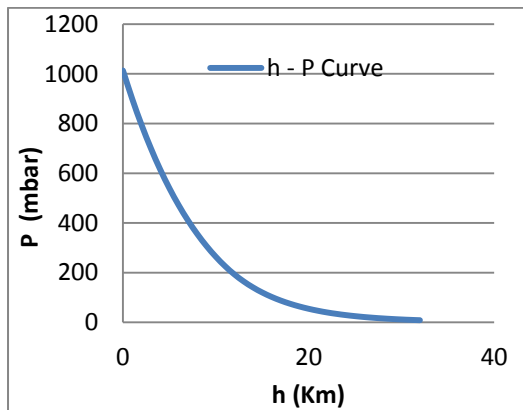


Fig (2) shows the pressure P(mbar) varies with altitude h (km)

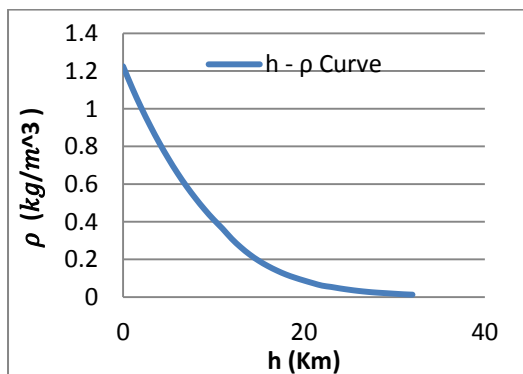


Fig (3) shows the density ρ (kg/m³) varies with altitude h (km)

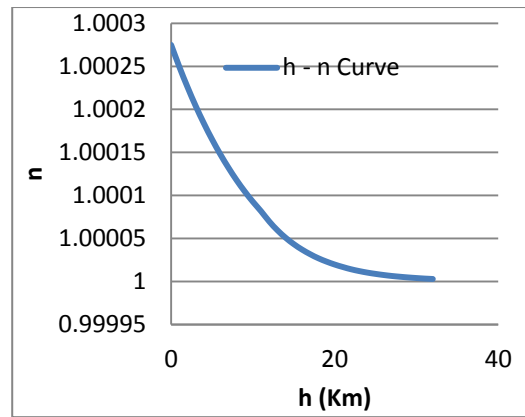


Fig (4) shows the refractive index decreases in exponential function with increasing altitude.

The negative gradient in values T and ρ causes variation in the refraction index n (Eqs. 7,8). Fig.4 shows the refractive index decreases in exponential function with increasing altitude. In troposphere layer, the laser beam of weapon is affected by attenuation due to variation of n. In high altitudes the refractive index n approaching to 1 in order to decrease the density and changing the slight temperature (as shown in Figs 5,6), which leads to consider the middle of stratosphere, homogeneous and suitable for the work of laser weapons.

Based on the above, the refractive index structure constant C_n^2 is inversely proportional with altitude as shown in Fig.7, C_n^2 is a tool to measure the strength of atmospheric turbulence and an increase in C_n^2 value yields an increase in atmospheric turbulence, at MSL the $C_n^2 \approx 10^{-12} m^{-2/3}$ (during day and strong turbulence conditions).

The Fried parameter r_0 parameter defines a circular diameter over which the laser beam maintains coherence. Fig.8 shows the relation between r_0 and C_n^2 , a lower r_0 value implies stronger turbulence. For wavelength ($\lambda = 1.075 \mu m$) and target ranges for laser weapons, r_0 can range from strong turbulence 0.975 cm (at MSL) to weak turbulence 1.23565 cm at 32 km (middle of stratosphere) (as shown in Fig.9)

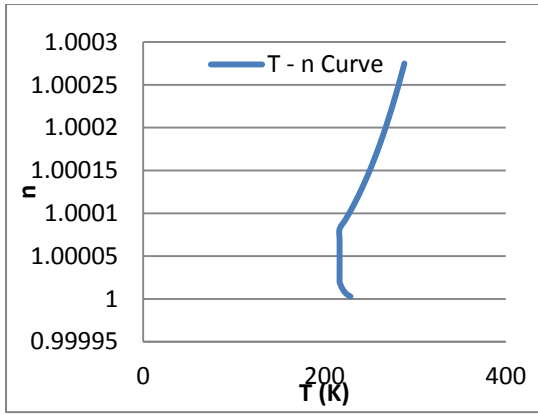


Fig (5) shows the refractive index decreases with increasing temperature.

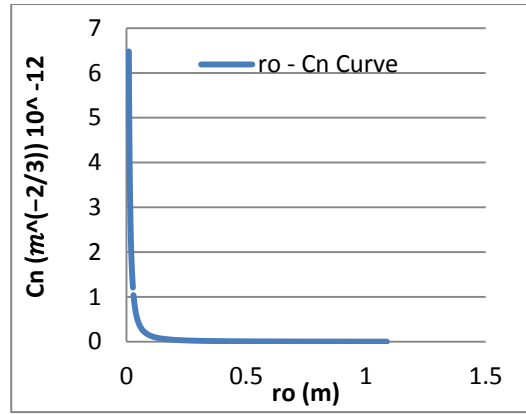


Fig (8) shows the relation between r_o and C_n^2

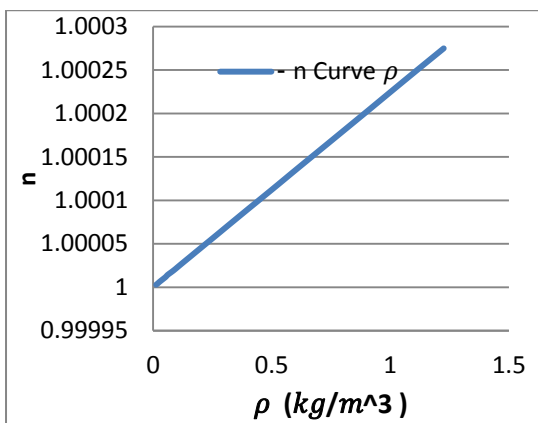


Fig (6) shows the refractive index increases with increasing density.

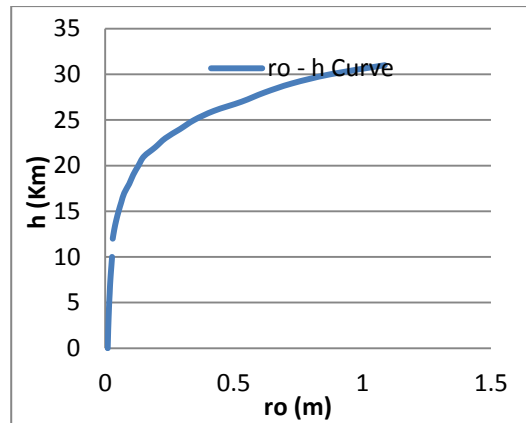


Fig (9) shows the relation between r_o and altitude

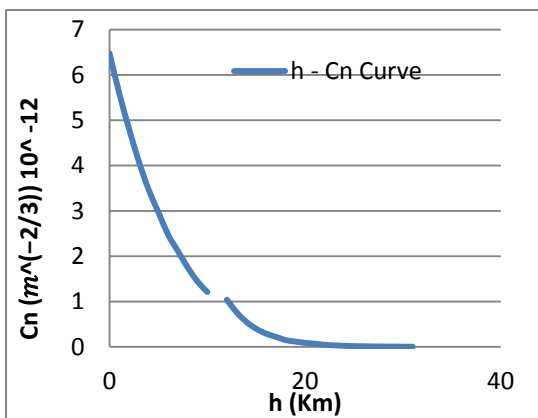


Fig (7) shows the refractive index structure constant C_n^2 is inversely proportional with altitude

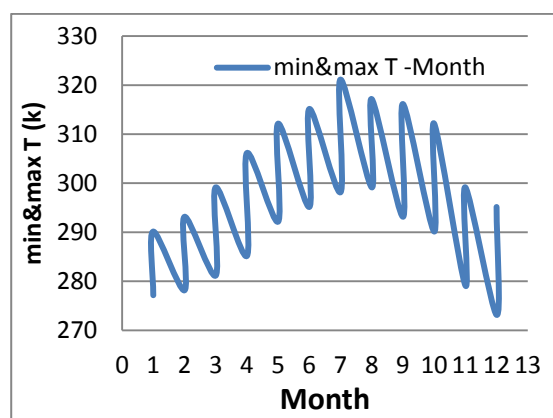


Fig (10) shows the curve of T for every month in year 2015

In Baghdad – Iraq, the change of temperature varies from season to season and also differs in one day. Table (3) shows the rate of change in refractive index as a result of the temperature difference at sea level. Fig.10 shows the variation in temperature minimum and maximum recorded in Baghdad on different months of the year (2015). It is clear that the July record the highest average temperature, as well as there is a variation in temperature in one day. This

variation in temperature will lead to a variation in the P, n and C_n^2 as shown in Figs. 11, 12, 13 respectively. It is noted, the greatest variation in the C_n^2 recorded in the October as a result of the transition from summer to winter. Thus, the laser beam will be affected negatively as a result of rising temperatures rates in Iraq and the consequent increase in Atmospheric turbulence.

Table (3): shows the rate of change in refractive index as a result of the temperature difference at sea level In Baghdad – Iraq (2015). [16]

month	T(k)	P(mbar)	Wind (m/s)	n	$C_n^2 (m^{-2})$
January	Min: 277.15	825.78	2.6	1.0002495	11.34×10^{-12}
	Max:290.15	1050.76		1.0002831	21.72×10^{-12}
February	Min: 278.15	841.57	2.9	1.0002366	35.21×10^{-12}
	Max:293.15	1109.14		1.0002958	23.33×10^{-12}
March	Min: 281.15	890.38	3.2	1.0002476	56.35×10^{-12}
	Max:299.15	1233.77		1.0003225	35.56×10^{-12}
April	Min: 285.15	959.01	3.2	1.0002630	86.70×10^{-12}
	Max:306.15	1393.62		1.0003559	37.13×10^{-12}
May	Min:292.15	1089.39	3.3	1.0002951	83.92×10^{-12}
	Max:312.15	1542.90		1.0003865	67.55×10^{-12}
June	Min: 295.15	1149.49	3.9	1.0003045	96.48×10^{-12}
	Max:315.15	1622.45		1.0004025	71.90×10^{-12}
July	Min: 298.15	1212.24	4	1.0003179	146.84×10^{-12}
	Max:321.15	1802.10		1.0004388	146.11×10^{-12}
August	Min: 299.15	1217.63	3.4	1.0003182	91.24×10^{-12}
	Max:317.15	1677.3		1.0004135	139.17×10^{-12}
September	Min: 293.15	1109.14	3	1.0002958	126.46×10^{-12}
	Max:316.15	1649.69		1.0004080	156.72×10^{-12}
October	Min: 290.15	1050.76	2.6	1.0002831	107.40×10^{-12}
	Max:312.15	1542.90		1.0003865	215.02×10^{-12}
November	Min: 279.15	857.59	2.5	1.0002402	68.04×10^{-12}
	Max:299.15	1233.77		1.0003225	107.61×10^{-12}
December	Min: 273.15	765.03	2.5	1.0002190	73.43×10^{-12}
	Max:295.15	1149.49		1.0003045	30.38×10^{-12}

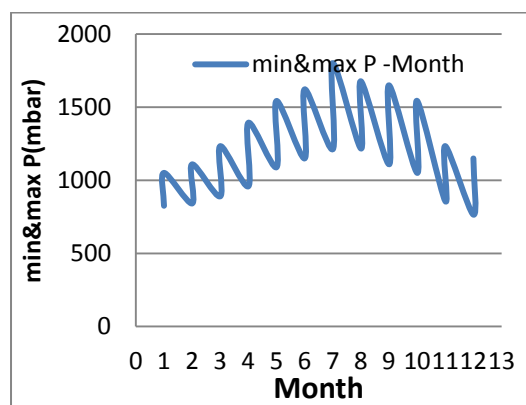


Fig (11) shows the curve of pressure for every month in year 2015

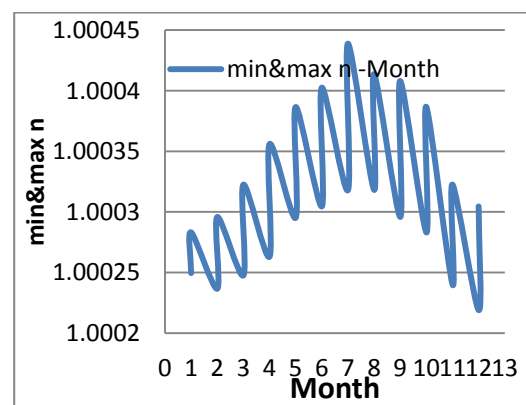


Fig (12) shows the curve of n for every month in year 2015

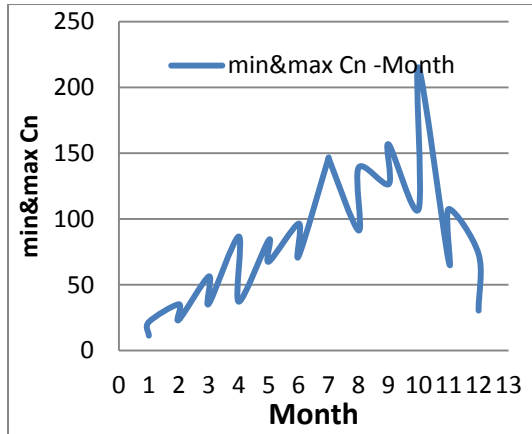


Fig (13) shows the curve of C_n^2 for every month in year 2015

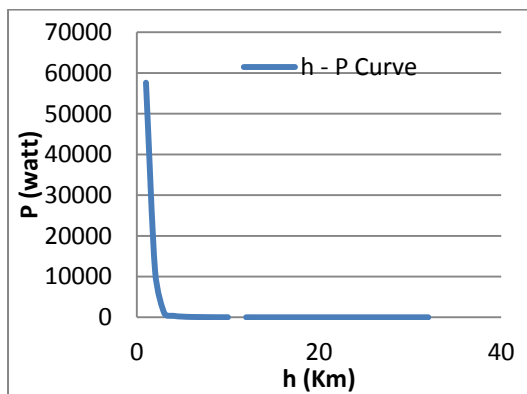


Fig (14) shows the power P (in watt) of laser beam is Inversely proportional with altitude h(km).

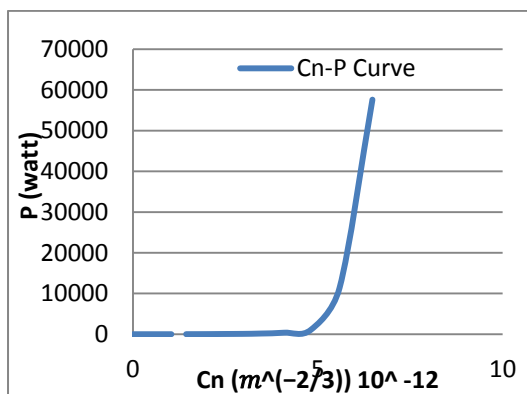


Fig (15) shows the curve of power P (in watt) of laser beam versus C_n^2

Finally, Table 4 shows the effect of turbulence attenuation and calculating the decrease of power P of laser weapon in Iraq. The laser beam interactions with the particles in the atmosphere (both molecules and aerosol particles), the laser beam will have many distorted

terms such as random time delay, pulse spread, beam wander. Fig. 14 shows the power P (in watt) of the laser beam is Inversely proportional with altitude h(km). Where most of the Power lost when crossing the troposphere and fade almost at the beginning layer of the stratosphere.

Table (4): shows the effect of turbulence attenuation and calculating the decrease of power P of laser weapon in Iraq

d (km)	q	ϵ (km^{-1})	r_0	R_s	P
1	0.585	2.620	0.01065	0.0351	57615.43
2	0.735	1.195	0.01166	0.0702	11372.54
3	0.840	0.742	0.012857	0.1053	1054.78
4	0.924	0.526	0.01419	0.1404	377.04
5	0.994	0.401	0.01557	0.1755	170.51
6	1.05	0.322	0.01740	0.2106	88.45
7	1.3	0.233	0.01912	0.2457	64.51
8	1.3	0.204	0.02139	0.2809	37.75
9	1.3	0.181	0.02405	0.3160	23.64
10	1.3	0.163	0.0267	0.3511	15.49
11	1.3	0.148	End of Troposphere		
12	1.3	0.136	0.02924	0.4213	7.45
13	1.3	0.125	0.03529	0.4564	5.45
14	1.3	0.116	0.04285	0.4915	4.05
15	1.3	0.109	0.05203	0.5267	3.04
16	1.3	0.102	0.06265	0.5618	2.35
17	1.3	0.096	0.07405	0.5969	1.85
18	1.3	0.090	0.09344	0.6320	1.49
19	1.3	0.086	0.10896	0.6671	1.18
20	1.3	0.081	0.12921	0.7022	0.97
21	1.3	0.077	0.15034	0.7373	0.80
22	1.3	0.074	0.19425	0.7724	0.66
23	1.3	0.071	0.23392	0.8076	0.55
24	1.3	0.068	0.29089	0.8427	0.46
25	1.3	0.065	0.34631	0.8778	0.39
26	1.3	0.062	0.42318	0.9129	0.34
27	1.3	0.060	0.53020	0.9480	0.31
28	1.3	0.058	0.61898	0.9831	0.25
29	1.3	0.056	0.72614	1.0182	0.22
30	1.3	0.054	0.87437	1.0534	0.19
31	1.3	0.052	1.08742	1.0885	0.17
32	1.3	0.051	1.23565	1.1236	0.14

It is clear, that the effective range of laser weapon in Iraq does not exceed a few kilometers as a result of higher attenuation that occurs to the laser beam due to high temperatures as shown in Fig.15.

Conclusions:

1. The middle of stratosphere considered as a homogeneous and a suitable area for the work of laser weapons, so is a favorite area of fighter aircraft.

2. The effectiveness of laser weapons in Iraq severely affected due to large change in temperatures.
3. The effective range of laser weapon in Iraq does not exceed a few kilometers as a result of higher attenuation.
4. The greatest variation in the C_n^2 recorded in the October as a result of the transition from summer to winter.
5. The refractive index structure C_n^2 is affected by microclimate conditions, propagation path, season and time of day.
6. The value of C_n^2 in Iraq, grades ranging from strong $6.48 \times 10^{-12} m^{-\frac{2}{3}}$ at sea level to the weak $2.51 \times 10^{-15} m^{-\frac{2}{3}}$ at 31 km.

References:

- [1] John, E. O. 1987. Standard Atmosphere. Springer US, USA. PP 801.
- [2] Ashish T. 2007. Atmospheric and Space Flight Dynamics. Springer Science & Business Media, USA. PP 556.
- [3] Glenzer, S.H. and Froula, D.H. 2011. Laser Beam Propagation Through Long Ignition Scale Plasmas on NIF. IEEE International Conference on Plasma Science Monterey, USA.
- [4] Davies, M. 2003. The Standard Handbook for Aeronautical and Astronautical Engineers. McGraw-Hill standard handbooks, USA. PP 1360.
- [5] David, B. 2013. Analysis of Joint Effects of Refraction and Turbulence on Laser Beam Propagation in the Atmosphere. MSc Thesis, The School Of Engineering of The University Of Dayton, Ohio, USA. PP 56.
- [6] Andrew, L. P. 2011. Optical Communication Through the Turbulent Atmosphere with Transmitter and Receiver Diversity. Ph.D Thesis, Stanford University, Massachusetts Institute Of Technology. USA. PP 256.
- [7] Ronald, O. R. 2015. Navy Shipboard Lasers for Surface, Air, and Missile Defense: Background and Issues for Congress, Congressional Research Service Congress, USA.
- [8] Dainty, J. C. 2009. Optical Effect of Atmospheric Turbulence, Springer Netherlands, London UK. pp 1-22.
- [9] Fussman, C. R. 2014. High energy laser propagation in various atmospheric conditions utilizing a new, accelerated scaling code. Ph.D. Thesis, Monterey, California: Naval Postgraduate School, USA. PP 114.
- [10] Aleš, P. 2009. Modeling of Atmospheric Turbulence Effect on Terrestrial FSO Link, Radioengineering, Czech Republic 18(1): 42-47.
- [11] Jan, S. and Götz, N. 2010. Assessment of Long Range Laser Weapon Engagements: The Case of the Airborne Laser, Science and Global Security, 18(1): 1-60.
- [12] Keith, J. R. 2012. Evaluation and Design of Non-Lethal Laser Dazzlers Utilizing Microcontrollers. MSc Thesis, B.S. Mechanical Engineering, University of Kansas. USA. PP 126.
- [13] Lucie, D. and Otakar, W. 2009. Laser Beam Attenuation Determined by the Method of Available Optical Power in Turbulent Atmosphere. Journal of Telecommunications And Information Technology. 2(1): 53-57
- [14] Varanasi, S. L.; Subba, S. S. and Sistu, R. 2013. Effects of weak atmospheric turbulence on FSO link Systems and its reducing technique. International Journal of Advancements in Research & Technology. 2(11): 213-226.

- [15] Hakan, U. 2004. Spot Size, Depth of Focus, and Diffraction Ring Intensity Formulas For Truncated Gaussian Beams, Paper, Applied Optics Journal , 43(3): 620-625
- [16] Accuracy Weather company. 2015. Weather for Life, Weather in Baghdad, Iraq.

تحليل ودراسة تأثير الاضطرابات الجوية على سلاح الليزر في العراق

مدرس ثائر عبد الكريم خليل العايش

قسم الفيزياء، كلية التربية ابن الهيثم، جامعه بغداد، بغداد، العراق.

الخلاصة:

واحدة من أهم التحديات التي تواجه تطوير أسلحة الليزر تتمثل بالتوهين الحاصل لحزمة الليزر أثناء مرورها خلال طبقات الغلاف الجوي. هذا البحث قدم دراسة نظرية لمحاكاة تأثير توهين الاضطرابات واحتساب انخفاض قوة الليزر في العراق. ان معامل الانكسار الهيكلي C_n^2 مهم جدا لقياس قوة من الاضطراب في الغلاف الجوي، والذي يتأثر بتغير الظروف المناخية ومسار الانتشار والموسم والتوقيت في اليوم الواحد. نتائج القياسات والتنبؤات مبنية على نظرية الاضطراب كولموجوروف. وقد تبين من خلال المحاكاة، ان فعالية أسلحة الليزر في العراق تتأثر كثيرا بسبب التغير الكبير في درجات الحرارة، وان المدى الفعال لسلاح الليزر لا يتجاوز بضعة كيلومترات نتيجة للتوهين العالي، وان انسب منطقة متجانسة لعمل اسلحة الليزر هي منتصف طبقة الستراتوسفير، لذلك تمثل منطقة مفضلة للطائرة المقاتلة.

الكلمات المفتاحية: توهين الاضطراب، سلاح الليزر، معامل الانكسار الهيكلي C_n^2 ، معامل فريد r_0 ، انقراج الحزمة.